Novel probabilistic crack growth assessment method: Based on the realised PDF law for growing cracks

Saifi, Qais

Published in:
Engineering Fracture Mechanics

DOI:
10.1016/j.engfracmech.2022.108931

Published: 01/12/2022

Engineering Fracture Mechanics 276 (2022) 108931

Contents lists available at ScienceDirect

Engineering Fracture Mechanics

journal homepage: www.elsevier.com/locate/engfracmech

Review

Novel probabilistic crack growth assessment method: Based on the realised PDF law for growing cracks

Qais Saifi

VTT Technical Research Centre of Finland Ltd, Kemistintie 3, Espoo, P. O. Box 1000, FI-02044 VTT, Finland

A R T I C L E I N F O

Keywords:
Probability density function
Finite cell weight variation method
Probabilistic crack growth assessment
Initial crack size distribution

A B S T R A C T

Probabilistic fracture mechanics (PFM)-based crack growth assessment in load-bearing components has become a robust tool for reliability estimation for several decades. The PFM assessment considers at least one input parameter probabilistically distributed to estimate crack size probability over time. Nonlinear crack growth over time is primarily responsible for the high computational cost in PFM assessments. This paper establishes a novel probability density function (PDF) law for nonlinearly growing cracks. Furthermore, this law enables the development of the finite cell weight variation (FCWV) method as an efficient probabilistic crack growth procedure. The FCWV method discretises an input PDF parameter into a finite number of cells along the random variable axis and ties a crack size to every cell boundary. Consequently, the FCWV method determines the probability of crack size over time by computing the crack sizes at the cells' boundaries. The crack size probability at every cell remains constant, whereas their PDFs vary over time because of non-linear crack growth. This paper considers a pipe susceptible to stress corrosion cracking with a circumferential semi-elliptical inner surface crack for validation. The initial crack length is postulated as the only probabilistically distributed input parameter. The FCWV with 20 cells and Latin hypercube sampling with 10,000 samples are applied to determine the probability of crack size over time. The results from both methods are in excellent agreement. Thus, such quantitative results prove the computational efficiency of the FCWV method, because the number of cells or samples is equivalent to the number of calculations a computer performs at a time step.

1. Introduction

The piping systems and mechanical components of a nuclear power plant (NPP) start ageing degradation at the beginning of their service life. In terms of degradation modes, crack initiation and growth as a function of time cause one of the most significant ageing effects for NPP components. The material, environment and loading conditions of these components are crucial for possible crack initiation and growth [2]. Typically, to optimise the risk-informed in-service inspection (RI-ISI) or long-term operation (LTO) of components susceptible to crack growth ageing, NPP operators apply their probabilistic risk assessment programme to assess leak and failure probabilities [1,5,7]. Leak and failure probabilities can be assessed computationally by applying probabilistic fracture mechanics (PFM)-based models. In a PFM model, a crack may initiate and grow with a probability in a component under the influence of active degradation mechanisms for given component materials, loads and environments. Stress corrosion cracking (SCC), fatigue and corrosion fatigue are the typical degradation mechanisms that cause crack initiation and growth. Significant papers have shown

E-mail address: mir.saifi@vtt.fi.

https://doi.org/10.1016/j.engfracmech.2022.108931
Received 3 May 2022; Received in revised form 25 September 2022; Accepted 7 November 2022
Available online 18 November 2022

examples of handling these degradation mechanisms experimentally and computationally [16–19]. The activation of these degradation mechanisms in a mechanical component requires a certain combination of material, environment and loading conditions. Before crack growth occurs, a crack generally takes some time (months or even years) to incubate or initiate. This time can be determined probabilistically as a function of material, environment and loading conditions [20]. However, the probabilistic assessment of crack initiation is computationally a much lighter task than crack growth. PFM tools are applicable for performing probabilistic crack growth assessments. A PFM methodology is computationally cumbersome for two main reasons. First, the nonlinear nature of crack growth requires a stepwise assessment over time. Hence, PFM assessment is performed by using discrete time steps if the analysed component is susceptible to SCC (load cycles apply in the case of fatigue). Second, input parameters related to material, loading, environment and initial crack size can be available in a probabilistic format. Performing a PFM assessment with several probabilistic input parameters over a large number of time steps is indeed computationally cumbersome. In addition to input parameters, nonlinear crack growth depends on crack size history. Except for crack size, all other input parameters only cause the crack to grow. The dependency of crack growth on crack size history makes this parameter both a cause and an effect. Consequently, one can associate a single combination of randomly picked input parameters with a single crack size and its growth history. In a PFM assessment, the shape of probabilistic crack size distribution changes over time because of nonlinear crack growth [21]. Thus, solving the probabilistic crack size distribution over time is a primary problem for computational efficiency. Other probabilistic input parameters are secondary problems, as they can be associated with the primary problem. A procedure for solving the primary problem can be applied to solving the secondary problem. In ref. [21], only the material parameter was probabilistic in fatigue crack growth experiments. The shape of the crack size distribution varies over time (load cycles). Every randomised material parameter can be associated with a crack size, where all crack sizes have a single initial deterministic value (see Figure 5 of ref. [21]).

Any attempt to develop a probabilistic crack size assessment procedure must consider the initial crack size as a probabilistically distributed input parameter. Indeed, probabilistic initial crack size is the primary parameter that may significantly affect crack size distribution results over time compared to any other input parameter; it may even limit the applicability range of a developed procedure. Moreover, other input parameters can be determined conservatively in analysing hundreds of components for the RI-ISI or LTO programme, except for the initial crack size. Thus, the initial crack size is one of the most common uncertain or probabilistic input parameters in a PFM analysis. Other often probabilistically considered parameters in the PFM analysis are material properties, loading and environment. However, these parameters may or may not be considered uncertain.

In general, the measured data of a probabilistically distributed parameter are often fitted to a suitable probability density function (PDF). PDFs for different parameters are inverted to their respective cumulative distribution functions (CDFs), and parameter samples are obtained from those CDFs. Eventually, crack growth analyses are performed with all samples of all parameters. For instance, if 1,000 initial crack samples and 1,000 environment samples are obtained, every crack sample will be analyzed for every environment sample, which means that 10^6 analyses will be performed. Classically, the Monte Carlo sampling (MCS) method was proposed in [15] to obtain parameter samples from a CDF. In an MCS, a computer picks pseudo-random numbers between 0 and 1. To maintain the probabilistic significance of a parameter, tens of thousands of MCS computations of the parameter are typically required. In PFM assessments, MCS has been commonly applied as a crude method for obtaining samples of probabilistic parameters [8,9,10,12]. Latin hypercube sampling (LHS) is a more efficient form of MCS. In LHS, a CDF is divided into a number of probability spaces with equal probability weights. Typically, a pseudorandom number is picked to obtain a sample within each probability space interval. LHS has been applied in numerous studies, such as articles and reports related to PFM assessments [4,9,10]. The importance sampling (IS) method is applied in PFM assessments to sample probabilistic parameters when an extremely low probability of rupture is expected. The IS method is biased MCS or LHS, where the simulation of the samples occurs at the tail of the PDF to obtain an extremely low probability of rupture adequately [10,12,13,14]. As an alternative to MCS and LHS in PFM assessment, discrete probability density (DPD) sampling was applied in refs. [13] and [14]. In a DPD analysis, CDF (or PDF) is discretised into a number of intervals with their associated probabilities, where each probability has a local mean value. The assessment was performed at the local mean values, and related probabilities were carried out during the analysis [14]. With the DPD method, several hundreds of samples for a probabilistic parameter typically suffice, compared to several thousands of samples needed when using LHS.

This paper proposes a novel probabilistic procedure for the PFM assessment of distributed crack growth. The procedure is developed based on providing a PDF law for probabilistic crack growth as a function of time and regenerating a new PDF for each time increment. For constant and linear growth rate of initial crack size over a distribution, analysis at only initial maximum and initial minimum crack sizes suffices to obtain all needed probabilistic information. However, crack growth is typically a non-linear phenomenon with a varying growth rate, where the stress distribution through the component wall, material properties and environment may significantly influence the growth rate. For PDF regeneration, to capture the influence of non-linear crack growth, the distributed initial crack size is discretised into a finite number of cells with initial weights. Constant probabilities are defined for each cell based on the realised law. However, the weight of the cells changes as a function of time. Thus, the PDF changes with respect to the finite cell weight variation (FCWV). The number of cells required in the FCWV method is of the order of several tens, compared to hundreds in DPD, thousands in LHS, and tens of thousands in MCS.

This paper considers a pipe susceptible to SCC with a circumferentially oriented semi-elliptical crack opening to the inner surface. The crack length and depth can fully describe the size of a semi-elliptical crack. Given that the initial crack size is the primary parameter, only this parameter is considered probabilistically distributed for validating the PDF law and the FCWV method. The validation is compared against an existing method, such as LHS. At the current stage, employing a semi-elliptical crack shape is essential for showing how the method works because of crack size constraints. Therefore, experimental data for validation of such crack shape are not available. An initial deterministic crack size will become probabilistically distributed over time for any other probabilistic input parameter. Thus, the PDF law and FCWV method will be applied if other parameters are defined probabilistically.

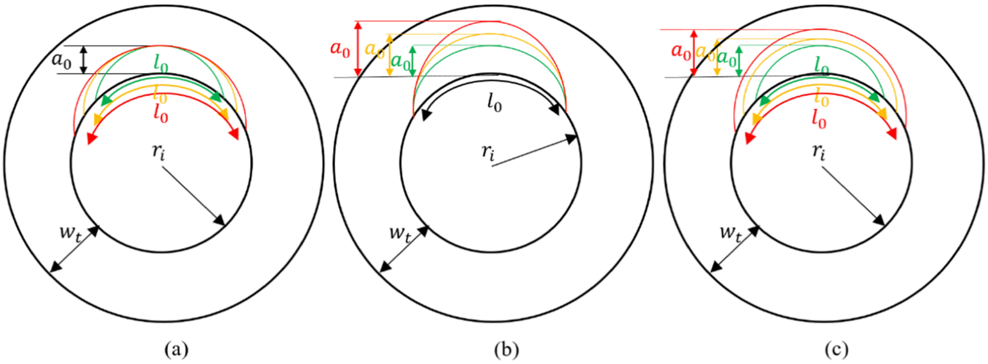

Fig. 2.1. Initial semi-elliptical circumferential cracks where, in size constraint, the smaller crack lays within the boundaries of the larger crack.

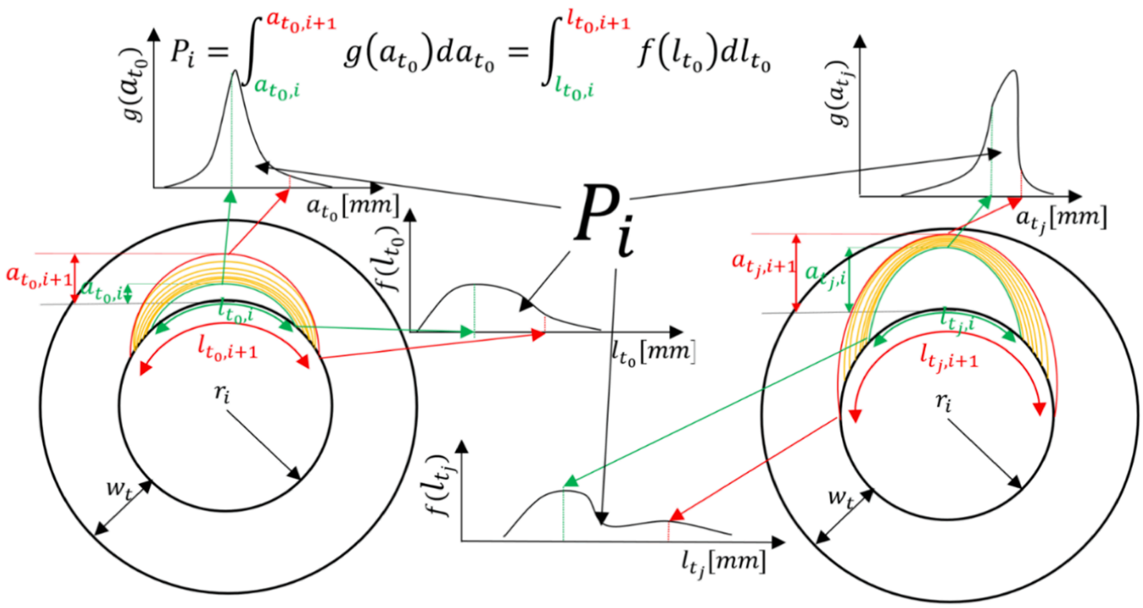

Fig. 2.2. Change in crack length and depth PDFs for cell i as a function of time for constant P_i.

Currently, other input parameters related to material and loading are assumed to be deterministic to avoid the paper becoming too long. However, in at least two more articles under planning, determining other parameters and their combinations probabilistically will be handled with the PDF law and the FCWV method.

2. FCWV method

The underlying assumptions behind the novel FCWV method for the same conditions (material properties, component cross-section geometry, environment and loads) are as follows:

- Continuous growth: Crack growth is continuous over time. The growth rate may continuously increase or decrease with respect to time (or stress cycles in the case of fatigue).
- Size constraint condition: For growing cracks over time, an initial smaller crack lying within the boundaries of an initial larger crack will always remain smaller and will lie within the boundaries of the larger crack. In Fig. 2.1, three cracks with different sizes for the three cases (a), (b) and (c) are shown. For all three cases, the orange and green cracks will never be larger than the red and orange ones at any given time. This is the initial crack size distribution limitation. The initial crack size distribution parameter is considered in this paper because of this limitation, and other input parameters lack such limitations.

Thus, the PDFs of the initial random crack depth and length continuously move to the right along the randomised variable axis over time due to continuous crack growth (crack depth and length are discussed in this paper, considering axisymmetric stress distribution through the wall of a hollow cylinder). However, the shape of PDFs or probability densities will change continuously over time due to nonlinear crack growth. As the area under the PDF curve is constant and equal to one at all times, contraction or expansion of the points along the random variable axis may occur. These factors cause an increase or decrease in the probability density. Contraction in the vicinity of a random point occurs at a given time when the growth rate of the random point is smaller than the growth rate of smaller random points in its vicinity. If the growth rate of the random point is higher than the growth rate of smaller random points in its vicinity, expansion at the vicinity of the point occurs. In a crack growth analysis, stress distribution normal to the crack face through the wall plays a crucial role in the contraction and expansion of random crack depths and lengths. If the stress distribution through the uncracked wall fluctuates between tensile and compressive stresses, the growth rate will increase and decrease over time for a growing crack. Thus, random cracks approaching the compressive or tensile region of the wall contract or expand along the randomised axis of the PDF because of a decrease or increase in the growth rates. Consequently, the PDF law for non-linearly growing cracks under similar conditions (material properties, component cross-section geometry, environment and loads) can be established as follows:

"An initial smaller crack laying within the boundaries of an initial larger crack in a plane will remain smaller at any given time and will not exceed the boundaries of the larger crack. Thus, the probability between two random cracks remains constant at any given time if initial random cracks are distributed so that a smaller crack lies within the boundaries of the next larger crack. However, the probability density between the random crack fronts along a given direction will increase or decrease due to the contraction or expansion of crack fronts along that direction.".

Fig. 2.2 presents the above-stated law in cylindrical cross-section with initial crack depth (crack fronts along the depth direction) and length (crack fronts along the length direction) PDFs, respectively, shown with letters g and f at initial time t_0. The cracks are inner surface-breaking semi-elliptical with a circumferential orientation, where crack depth and length can fully describe their size. A smaller crack lies within the boundaries of the next larger crack in Fig. 2.2, where the crack fronts with the green and red colours are the smallest and largest ones. Initial crack lengths and depths may have different distributions or PDFs, as shown in Fig. 2.2. Crack fronts may be more compact at the depth than at the length (or vice versa), resulting in a denser distribution in one location than in the other. However, selecting any random cell with lower and upper crack front boundaries will produce precisely the same probability at both depth and length by integrating their PDFs within the boundaries. This is because the total number of cracks within a boundary is the same at both depth and length. The red and green boundaries clearly produce a cell (i.e. i), where the crack distribution outside these boundaries is not shown in the cross-sections. Cell i has a constant probability P_i at all times at depth and length locations (e.g. Fig. 2.2) at times t_0 and t_j. Integrating any initial PDF (in this case length or depth direction) over the given red upper boundary and green lower boundary will result in P_i, as shown in Fig. 2.2. However, the probability densities change between the lower and upper boundaries over time because of nonlinear crack growth. Moreover, the change in the probability densities of the crack fronts along different directions can be different (e.g. crack fronts contract in the depth direction and expand in the length direction in Fig. 2.2 at time t_j). The contraction and expansion of the crack fronts along a given direction can be a local phenomenon at a given time for a complex stress field in the cracked plane. Crack fronts along the given direction may expand locally and contract at several locations, which will cause decreases and increases in the PDF at those locations. In NPP components, such complex stress fields are common in welded regions because of welding process-induced residual stresses. Discretising the PDFs of the crack fronts into a finite number of cells will capture local increases and decreases in PDFs over time for growing cracks. The probabilities of cells remain constant over time. Based on the PDF law of growing cracks, the finite cell weight will vary over time. Consequently, the probability density of the cell will vary, as shown in Fig. 2.2, and is derived as follows:

$$P_i = \int_{l_i}^{l_{i+1}} f_i(l(t))dl, \;\; l_i(t) \le l(t) \le l_{i+1}(t)$$

$$P_i = \int_{a_i}^{a_{i+1}} g_i(a(t))da, \;\; a_i(t) \le a(t) \le a_{i+1}(t), \;\; t > 0 \tag{2.1}$$

where l is the crack length, f_i is the PDF of crack length within the cell i, t is the time, a is the crack depth, and g_i is the PDF of crack depth within the cell i. By integrating the initial PDF within each cell, P_i is determined at $t = 0$ and kept constant over time. However, cell PDFs f_i and g_i change as crack lengths and depths respectively change over time (see Fig. 2.2 for crack length and depth).

2.1. Time-dependent PDFs based on trapezium approximation

In the simplest form, if a cell shape is approximated to a trapezium shape at any given time with a constant area (probability within that cell), then Eq. (2.1) can be rewritten as follows:

$$P_i \approx \frac{(f_{i,l_i} + f_{i,l_{i+1}})}{2}(l_{i+1} - l_i) = f_{i,m}w_{li,j} \Rightarrow f_{i,m} = \frac{1}{w_{li,j}}P_i, \; for \; w_{li,j} > 0$$

$$P_i \approx \frac{(g_{i,a_i} + g_{i,a_{i+1}})}{2}(a_{i+1} - a_i) = g_{i,m}w_{ai,j} \Rightarrow g_{i,m} = \frac{1}{w_{ai,j}}P_i, \; for \; w_{ai,j} > 0 \tag{2.2}$$

where subscript m is the midpoint of trapeziums, w is the weight of cells, subscript l is the crack length, subscript a is the crack depth, and subscript j is the time increment. The probability density of those cells for passing their limits of depth (or length) is obtained by summing their respective probabilities. For crack depth, the wall thickness is the limit, and for circumferential crack length, the inner circumference of the hollow cylinder is the limit. Thus, the probability density or probability at the limits is:

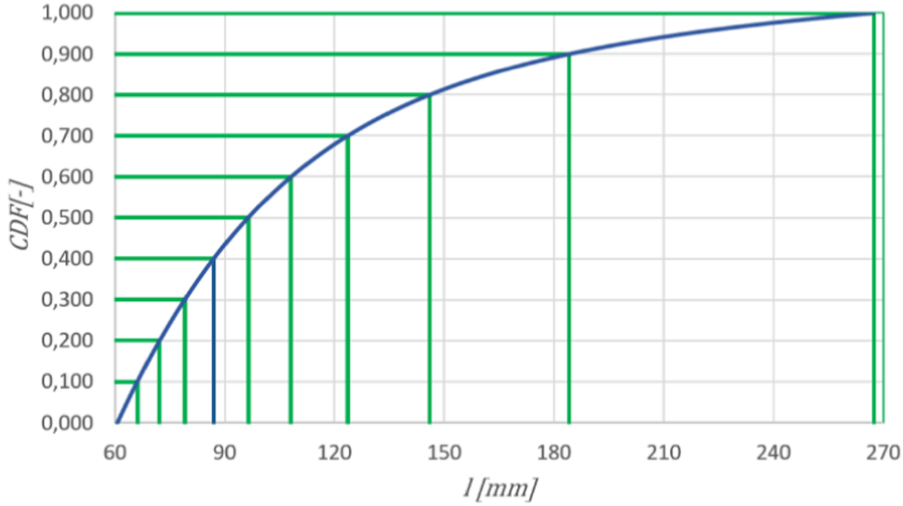

Fig. 2.3. Discretisation of the PDF into ten cells with equal probabilities and varying initial weights.

Table 1
Pipe cross-section and crack geometries.

r_i	w_t	a_0	l_0	NC
mm	mm	mm	mm	
51.13	6.02	0.5	Eq. (2.9)	20

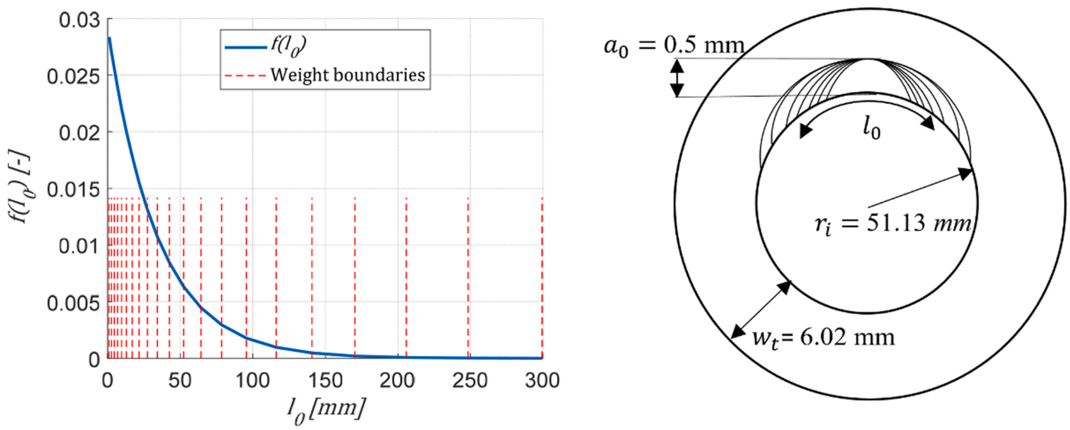

Fig. 2.4. Initial crack length distribution and PDF discretisation into 20 cells with initial boundaries of the cells (left) and geometrical dimensions (right).

$$P_{l_l} = f_{l_l} = \sum_{i=l_l}^{n} P_i, \; for \; l_{l_l, j_l} = l_{lim}$$

$$P_{a_l} = g_{a_l} = \sum_{i=a_l}^{n} P_i, \; for \; a_{a_l, j_a} = w_t \tag{2.3}$$

where subscript l_l and a_l denote the lower bound of a cell length and depth reaching their respective limits at their respective time increments. A crack length cell may reach its limit at a different time step than a crack depth cell. Thus, time subscripts j_l and j_a have been used to provide this distinction. If the limit resides in a cell, Eq. (2.2) can still be applied for current and upcoming time steps by artificially keeping the current w constant and allowing the lower bound to change over time until it reaches the limit.

With continuity conditions and trapezium shape approximation for the cells, the gradient of the probability density changes linearly for two adjacent cells between their midpoints as follows:

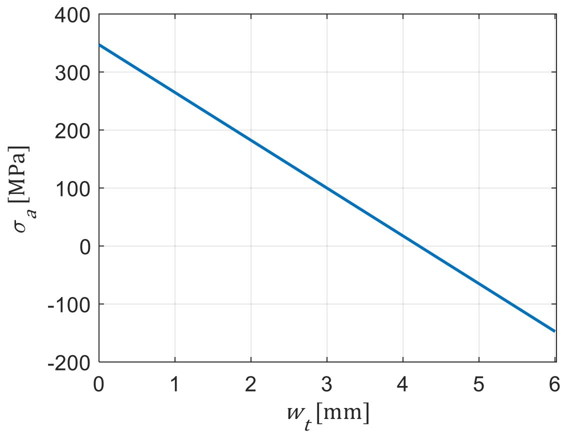

Fig. 3.1. Axial stress distribution through the wall of the pipe.

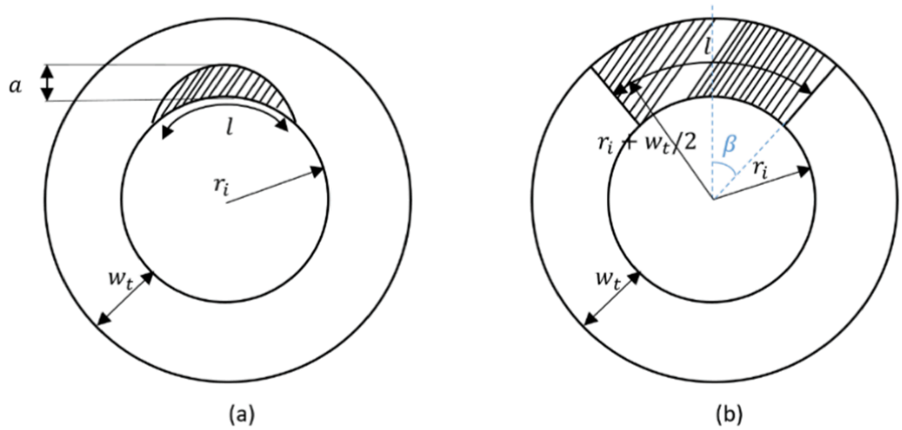

Fig. 3.2. Circumferentially oriented crack shapes in a cylindrical pipe, (a) semi-elliptical inner surface breaking crack, and (b) through-wall crack shape.

$$f \approx \frac{\left(f_{i+1,m}(t) - f_{i,m}(t)\right)}{\left(l_{i+1,m} - l_{i,m}\right)} w_l + f_{i,m}(t), \;\; l_{i,m}(t) \le l(t) \le l_{i+1,m}(t)$$

$$g \approx \frac{\left(g_{i+1,m}(t) - g_{i,m}(t)\right)}{\left(a_{i+1,m} - a_{i,m}\right)} w_a + g_{i,m}(t), \;\; a_{i,m}(t) \le a(t) \le a_{i+1,m}(t) \tag{2.4}$$

where the subscript m is for the midpoint (Eq. (2.2)). The cumulative probability up to a length, l_s, or depth, a_s, at a given time is defined as follows:

$$P_{l,c} = \int_{l_s}^{l_{i_l+1}} f(l)dl + \sum_{k=i_l+1}^{n} P_k, \;\; l_{il} < l_s \le l_{i_l+1}$$

$$P_{a,c} = \int_{a_s}^{a_{i_a+1}} g(a)da + \sum_{k=i_a+1}^{n} P_k, \;\; a_{i_a} < a_s \le a_{i_a+1} \tag{2.5}$$

where subscript i_l is the number of the cell where l resides currently, and subscript i_a is the number of the cell where a resides currently. PDF functions $f(l)$ and $g(l)$ can be defined from Eqs. (2.4) and (2.5). In Eq. (2.5), the cell probability accurately corresponds to a second-order polynomial at any cell, except for half of the two cells residing at the two ends of the distribution. The constant probability density must be assumed for end cells from their midpoints to their respective tails to avoid possible negative values by extrapolation. Constant probability densities for end cells from their midpoints to their respective tails are determined using Eq. (2.2). Thus, at these regions, the cell probability is first-order accurate.

The first-order PDFs of Eq. (2.4) may not be sufficiently accurate in the considered scenarios if:

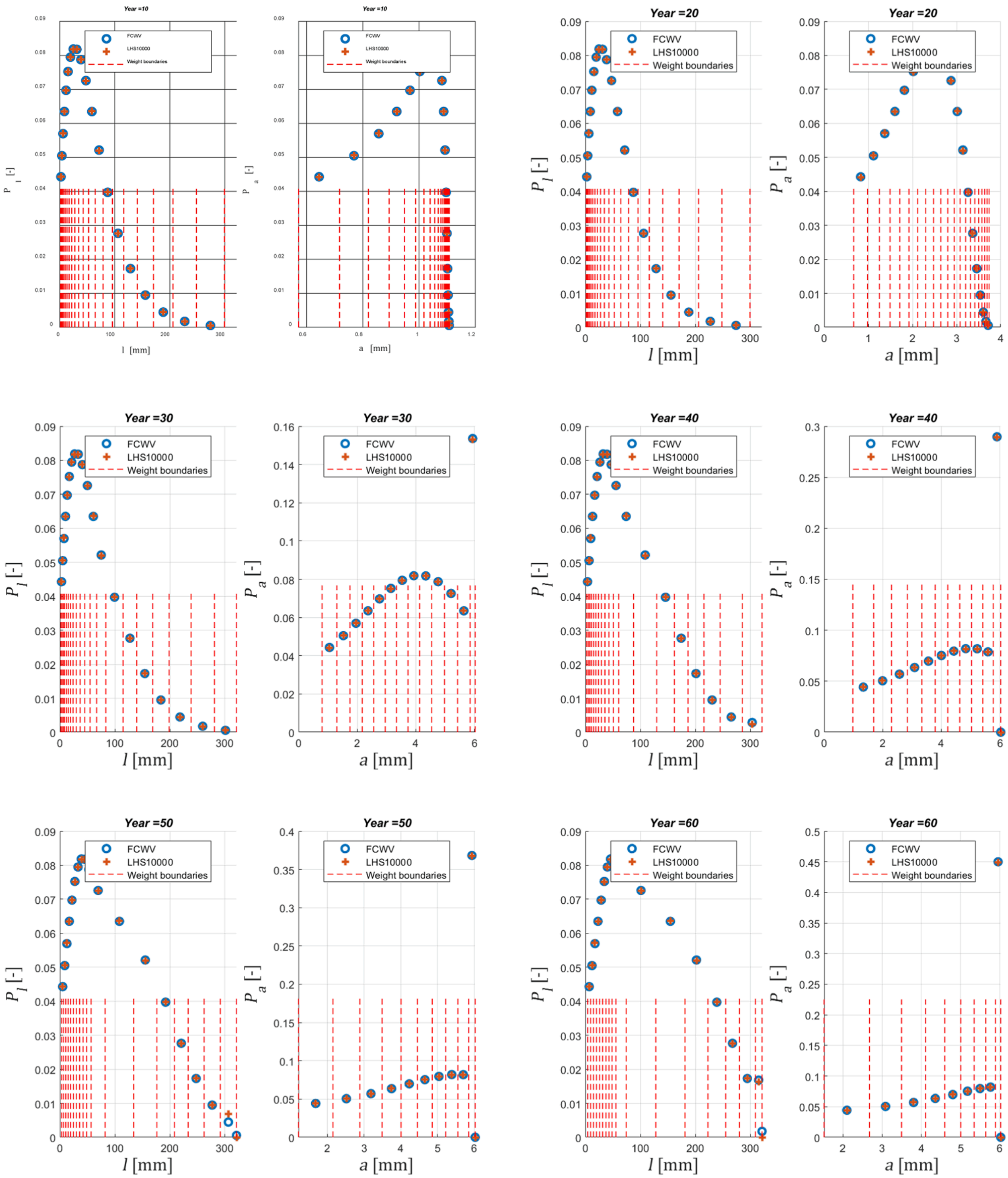

Fig. 4.1. Crack length and depth probabilities at different cells for different years.

- Extremely low probability is concerned (this usually happens at the tail, where PDFs are even considered constant),
- Very few numbers of cell discretisation are applied,
- Rapid crack growth is possible (in such a scenario, a deterministic assessment is usually performed to ensure fitness for service).

Thus, better approximations of PDFs are required for the above scenarios. A PDF fit to the exponential function is suggested in the following section, which is more accurate. However, this approximation may be computationally more expensive due to the associated convergence criteria.

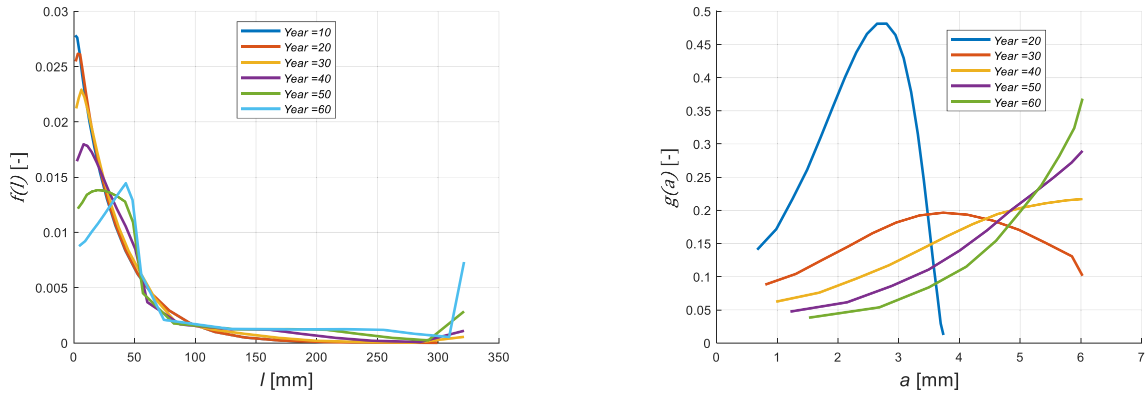

Fig. 4.2. PDFs of the growing crack length and depth at different years.

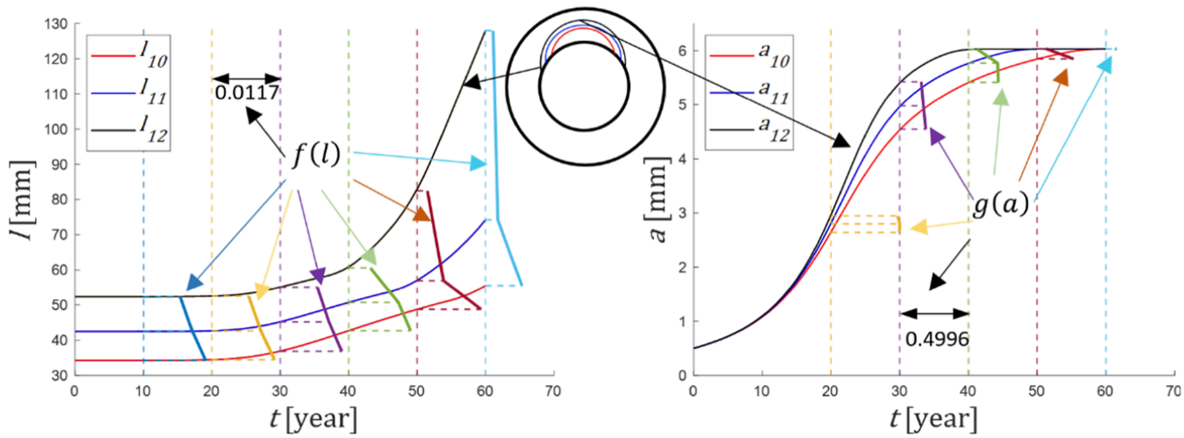

Fig. 4.3. Time-dependent PDFs at 10-year intervals and crack growth results at boundaries 10, 11 and 12 between cells 10 and 11.

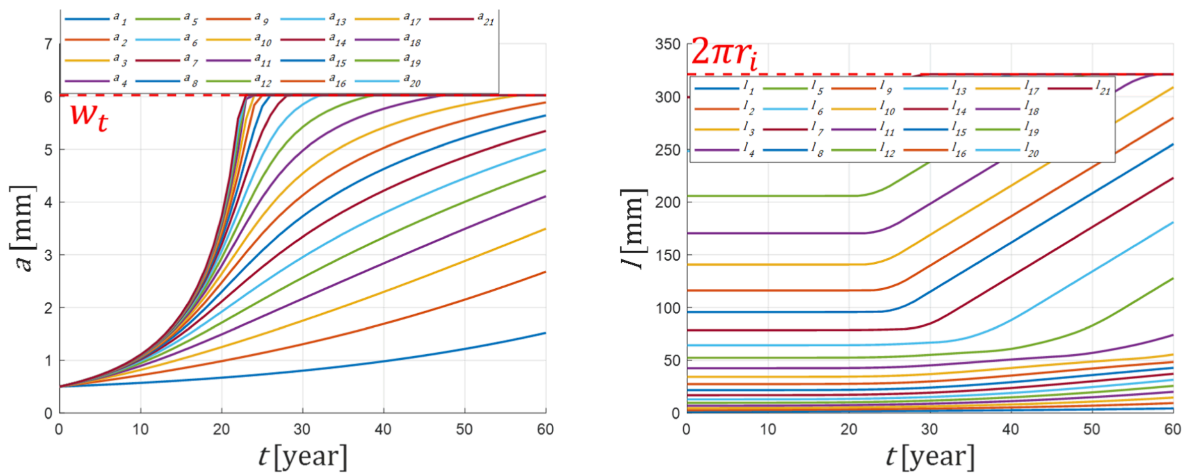

Fig. 4.4. Time-dependent crack growth results at all 21 boundaries.

2.2. *Time-dependent PDFs based on the exponential function*

Due to the non-linear nature of crack growth, the probability density within a cell may decay or grow exponentially at any given time, depending on a weight expansion or contraction from its initial state. Thus, an exponential function can describe the PDF of a cell

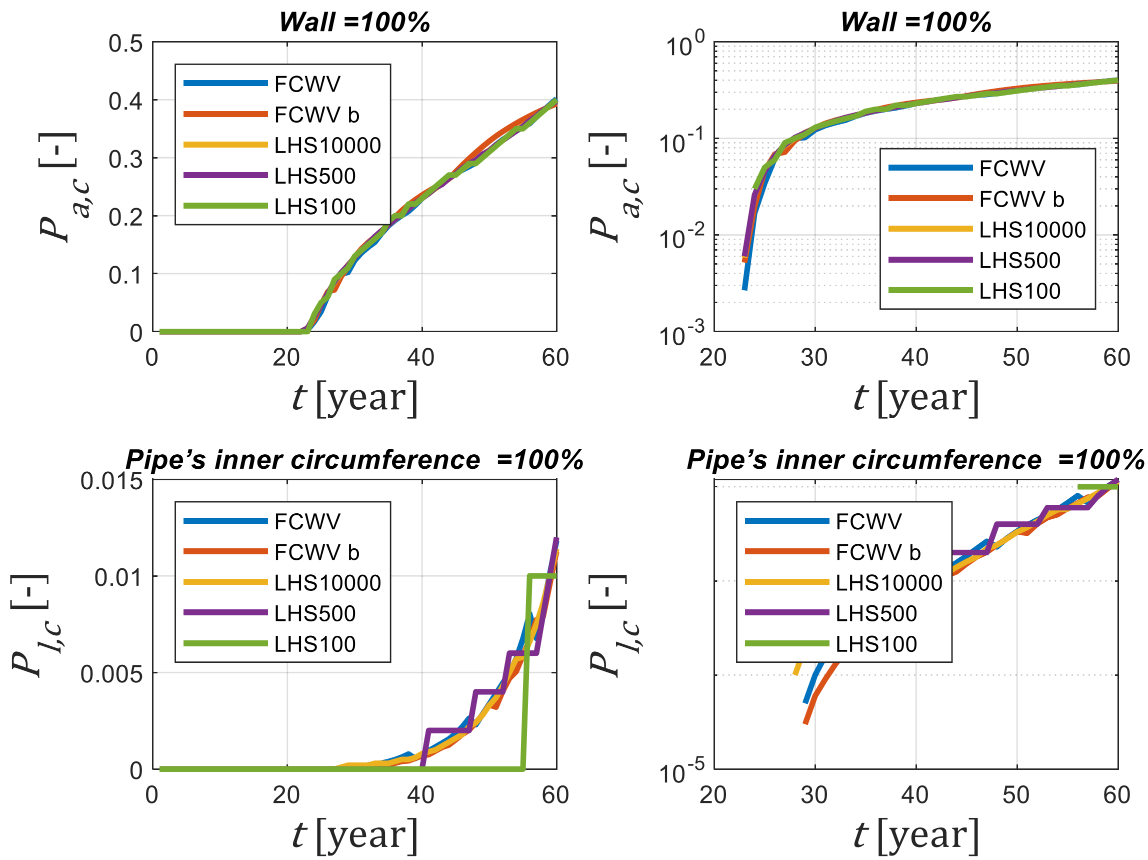

Fig. 4.6. Time-dependent cumulative probabilities of cracks reaching 90% of wall in the depth direction and 90% of inner circumference in the length direction.

well at any given time. Then, Eq. (2.1) can be rewritten as follows:

$$P_i = \int_{l_i}^{l_{i+1}} f(l)dl = \int_{l_i}^{l_{i+1}} exp\left(a_{l,i}l + b_{l,i}\right)dl, \;\; l_i(t) \le l \le l_{i+1}(t)$$

$$P_i = \int_{a_i}^{a_{i+1}} g(a)da = \int_{a_i}^{a_{i+1}} exp\left(a_{a,i}a + b_{a,i}\right)da, \;\; a_i(t) \le a \le a_{i+1}(t) \tag{2.6}$$

where parameters $a_{l,i}$ and $b_{l,i}$ are functions of the cell weight length $w_{li,j}$, and parameters $a_{a,i}$ and $b_{a,i}$ are functions of the cell weight depth $w_{ai,j}$. Parameters $b_{l,i}$ and $b_{a,i}$ can be defined by performing the integration of Eq. (2.6) and rearranging the results for these parameters as follows:

$$b_{l,i} = -a_{l,i}l_i + ln\left(\frac{P_i a_{l,i}}{exp\left(a_{l,i}w_{li,j}\right) - 1}\right), \;\; l_i(t) \le l(t) \le l_{i+1}(t)$$

$$b_{a,i} = -a_{a,i}a_i + ln\left(\frac{P_i a_{a,i}}{exp\left(a_{a,i}w_{ai,j}\right) - 1}\right), \;\; a_i(t) \le a(t) \le a_{i+1}(t) \tag{2.7}$$

See Eq. (2.2) for the weight of the cells $w_{li,j}$ and $w_{ai,j}$. Given that $a_{l,i}$ and $a_{a,i}$ are unknown, Eq. (2.6) for cells i and $i-1$ (previous cell next to cell i) can be integrated. By dividing P_i over P_{i-1}, the following functions are obtained, respectively, related to the crack length and the crack depth:

$$F\left(a_{l,i}\right) = exp\left(a_{l,i}\left(w_{li,j} + w_{li-1,j}\right)\right) - exp\left(a_{l,i}w_{li-1,j}\right)\left(1 + \frac{P_i}{P_{i-1}}\right) + \frac{P_i}{P_{i-1}} = 0$$

$$G\left(a_{a,i}\right) = exp\left(a_{a,i}\left(w_{ai,j} + w_{ai-1,j}\right)\right) - exp\left(a_{a,i}w_{ai-1,j}\right)\left(1 + \frac{P_i}{P_{i-1}}\right) + \frac{P_i}{P_{i-1}} = 0 \tag{2.8}$$

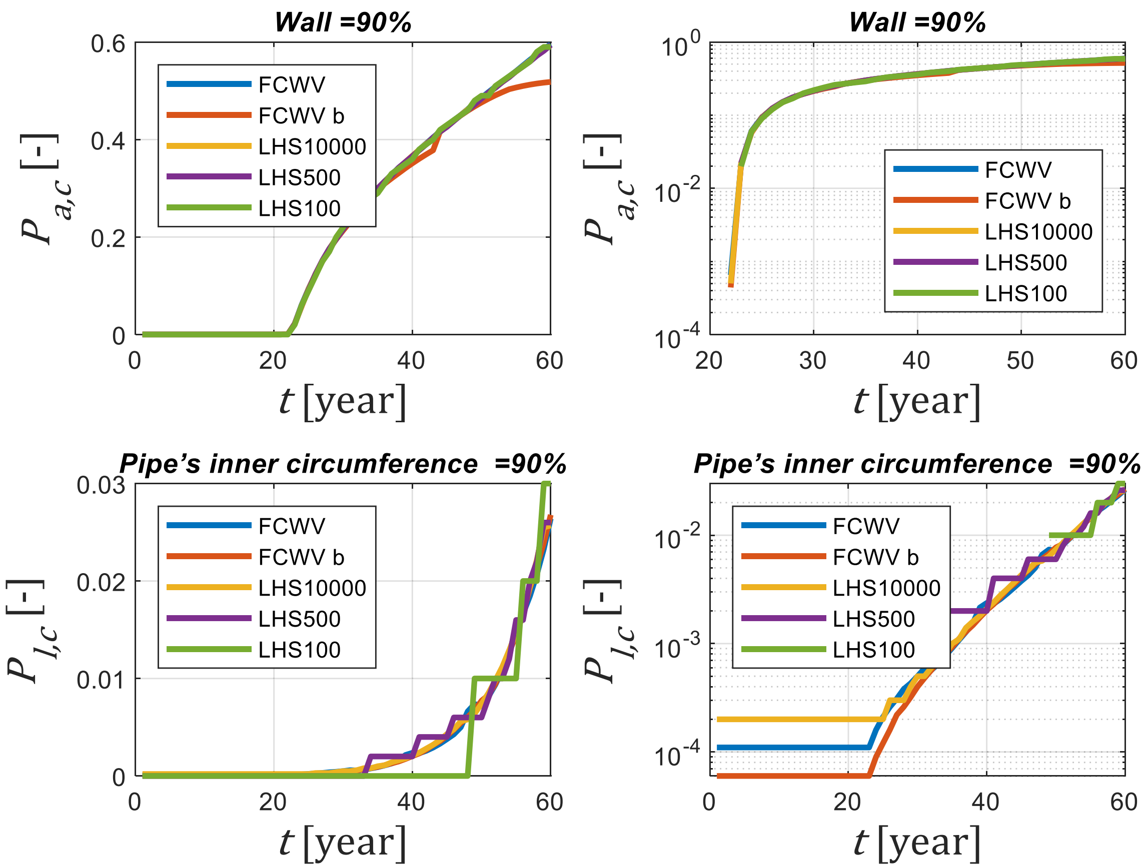

Fig. 4.5. Time-dependent cumulative probabilities of cracks reaching 100% of wall in the depth direction and 100% of inner circumference in the length direction.

Eq. (2.8) can be solved numerically for $a_{l,i}$ and $a_{a,i}$ by applying the Newtown method. In general, in the Newtown method, $a_{l,i}$ and $a_{a,i}$ are first guessed, and convergence criteria are set when $a_{l,i}$ and $a_{a,i}$ values from their respective previous iterations are very close to their current values. In this paper, Eqs. (2.6) and (2.7) are applied during the iteration process to compare P_i with the computed probability on the right-hand side of Eq. (2.6) for convergence. Thus, very few iterations are needed to achieve convergence without trading off accuracy. The smallest critical crack size lies only in one cell during leak, rupture or limit load probability assessments. This cell can be called the critical cell, where its lower boundary is safe and the upper boundary fails (see Fig. 2.2 for lower and upper boundaries of a cell). Therefore, regenerating the PDFs of the critical cell instead of all cells is sufficient. The critical cell number may change over time as cracks grow larger.

2.3. Cell discretisation and initial PDF

The desired discretisation method of the PDF into a finite number of cells is achieved by considering equal probabilities for each cell by inverting a PDF to a CDF (see Fig. 2.3 for the distributed crack length and depth). However, discretisation can be performed according to the regions of interest. This discretisation method is essential, especially in assessing extremely low probabilities or some other exceptional assessment cases.

In this paper, a circumferentially oriented semi-elliptical inner surface crack in a cylindrical cross-section is considered. The initial crack depth is assumed to be constant, and the initial crack length is distributed according to the following exponential PDF [3]:

$$f(l_0) = \frac{9.38}{2\pi r_i} e^{-\frac{9.38 l_0}{2\pi r_i}} \left(1 - e^{-9.38}\right)^{-1} H(2\pi r_i - l_0) \tag{2.9}$$

where l_0 is initial crack length, r_i is the inner radius of the pipe, and H is the Heaviside step function. The pipe cross-section and crack geometries are shown in Table 1.

In Table 1, w_t is the pipe wall thickness, a_0 is initial crack depth, and NC is the number of cells applied for the PDF discretisation. In this paper, cell discretisation is not done according to the equal probability method shown in Fig. 2.3. Instead, discretisation is done directly on the PDF curve. Fig. 2.4 shows the initial crack length distribution and the initial discretised cells along the length and geometrical dimensions. In this paper, we select an initial crack depth of 0.5 mm because it is a large enough depth that it may not be

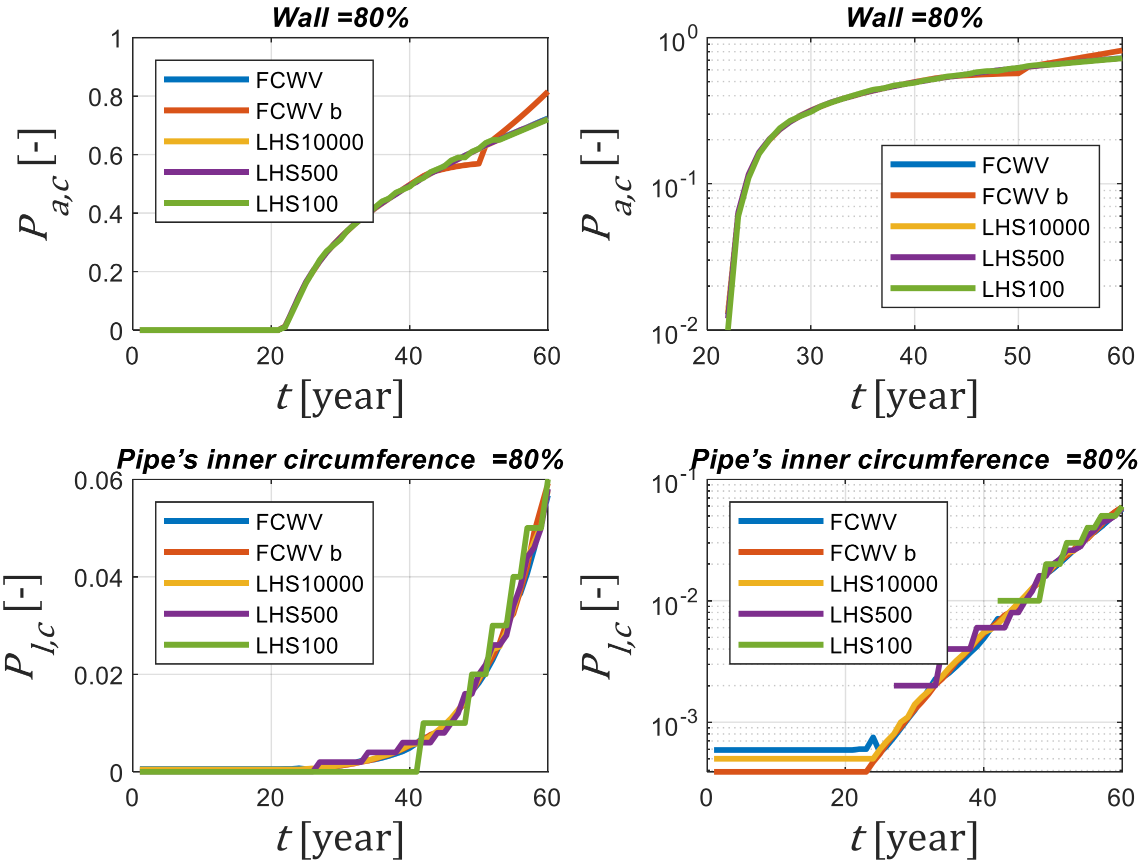

Fig. 4.7. Time-dependent cumulative probabilities of cracks reaching 80% of wall in the depth direction and 80% of inner circumference in the length direction.

detected with a high probability [22]. Therefore, analysing cracked pipes or components for the LTO programme can postulate such depths.

3. Crack growth

The analysed pipe is assumed to be a susceptible SCC damage mechanism. Circumferentially oriented semi-elliptical inner surface-breaking cracks are assumed to have been initiated already. The initial crack depth is assumed to be constant at 0.5 mm (see Section 2.3), and the initial crack length is distributed, as described in Table 1 and Fig. 2.4. Axisymmetric loading conditions are assumed for the pipe cross-section. Axial stress,σ_a, is assumed to be linearly distributed through the wall of the pipe (see Fig. 3.1).

The SCC growth rate for the length and depth of the crack is calculated as follows [4]:

$$\frac{dl}{dt} = 2CK_{I,l}^{n}$$

$$\frac{da}{dt} = CK_{I,a}^{n} \tag{3.1}$$

where l is the crack length, a is the crack depth, t is the time, and C and n are the material- and environment-dependent constants, respectively. $K_{I,l}$ and $K_{I,a}$ are mode I stress intensity factor at the surface and deepest points of the inner surface breaking semi-elliptical crack, respectively. The values for $K_{I,l}$ and $K_{I,a}$ are solved as a function of r_i, w_t, a, l, σ_a and material yield strength based on the solutions provided by ASME, Section XI [5]. Some of the distributed cracks may penetrate through the wall over time. Thus, instead of stress intensity factor solutions for semi-elliptical cracks, $K_{I,l}$ solution for the through wall cracks is needed. Moreover, $K_{I,a}$ is not needed for the through-wall cracks. $K_{I,l}$ solutions for the through wall cracks that are provided in ref. [6] as a function of w_t, l, σ_a and material yield strength are applied in this paper. Fig. 3.2 shows that circumferentially oriented semi-elliptical and through-wall cracks have cross-section and crack geometries.

In this study, the material parameter values in Eq. (3.1) are assumed as $C = 1.1^{-5}$ mm/(year(MPa$\sqrt{\text{m}}$)^n) and $n = 3$. Given that this study focuses on improving probabilistic crack growth assessment procedures over time, issues related to crack initiation, type of

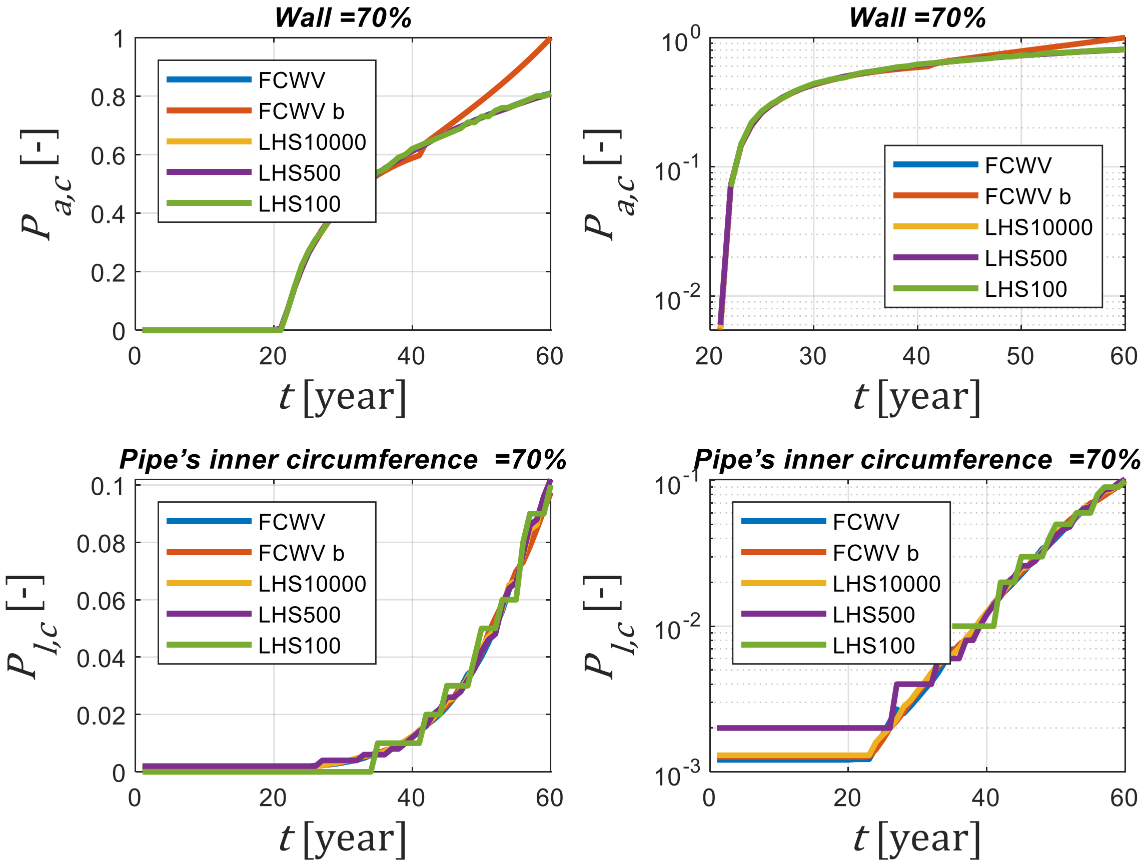

Fig. 4.8. Time-dependent cumulative probabilities of cracks reaching 70% of wall in the depth direction and 70% of inner circumference in the length direction.

degradation mechanisms, material, environment, loading conditions and applied crack solutions are irrelevant information. The proposed solution will be independent of such information. Here, some parameters are mentioned merely for convenience.

4. Results

The time-dependent probabilistic crack growth results obtained with the FCWV method using 20 cells are compared and validated with the LHS results. The probability results of the crack length, P_l, and the depth, P_a, at different cells at several time steps are shown in Fig. 4.1, where the FCWV results are compared to 10,000 LHS result points. Up to year 40, P_l and P_a results obtained with the FCWV method and 10,000 LHS points at different cells are almost identical. However, slight deviations in P_l results at the last cell in years 50 and 60 are observed. This is due to extrapolation of the $K_{I,l}$ solutions for larger crack sizes than the available solutions in ref. [6]. In addition to the weight changes of each cell over time for the crack lengths and crack depths, some cells disappear over time (see Fig. 4.1). The crack depth cells disappear faster because of the relatively thinner wall and significant inner surface stress (e.g. Fig. 4.1 shows that the number of crack depth cells is 20 in year 10 and 9 in year 60). The last six crack depth cells in year 30 have disappeared, and their probabilities have been added to the last cell near the wall (cell 13th).

Fig. 4.2 presents the computed PDF results for all the cells to see how the PDFs for crack length and depth evolve over time. However, the PDF results for all cells are not needed in the probabilistic leak or failure analysis. Obtaining PDFs only at the critical cell is sufficient because the probability within the cell until a critical point needs to be obtained by integration. The probabilities of succeeding cells are already known. In PDFs, the number of cells decreases over time as cells exceed their physical limit for crack length and crack depth (pipe circumference and wall thickness are assumed as the physical limits in this paper). The same cell number for crack depth and crack length have the same probability. However, their probability densities may differ. The current weights of the desired cell and the adjacent cell determine the probability density of the cell. Thus, the shape of the crack length and the crack depth PDFs change over time, seemingly independent of each other (indirectly, they are dependent through fracture mechanics-based crack analysis).

Fig. 4.3 shows the PDFs for cell number 10th and 11th at every 10-year interval. Crack depth and length results as a function of time for cell boundaries are also shown (i.e. boundaries numbered 11th, 11th and 12th). Fig. 4.4 shows the crack depth and length results over time for all boundaries.

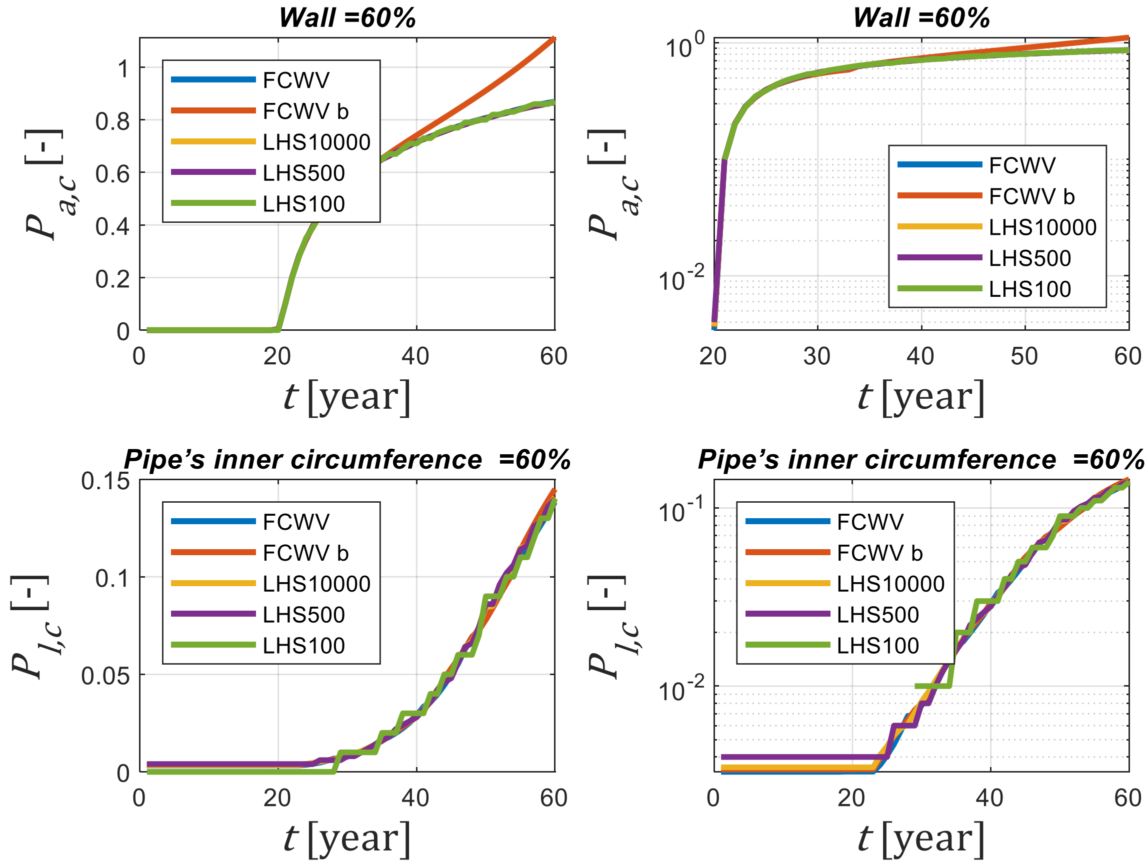

Fig. 4.9. Time-dependent cumulative probabilities of cracks reaching 60% of wall in the depth direction and 60% of inner circumference in the length direction.

The cumulative probabilities for cracks reaching certain depths and lengths are computed with the different numbers of the LHS result points for further validation of the FCWV method. Figs. 4.5 to 4.10 show the cumulative probability results for the crack depth, $P_{a,c}$, and the length, $P_{l,c}$, from five different computational assessments. In Figs. 4.5 to 4.10:

- "FCWV" presents the results from the FCWV method initially discretised according to the Fig. 2.4,
- "FCWV b" presents the results from the FCWV method discretised initially, with 20 cells having equal weights (not to be confused with equal probability in Fig. 2.3),
- "LHS 10000", "LHS 500" and "LHS 100" are for 10,000, 500 and 100 LHS result points, respectively.
- The right side plots are the same as the left side, except that the right side cumulative probability axis is logarithmic.

5. Conclusion

The PDF law for growing cracks has been realised under *continuous growth* and *size constraint* conditions. The FCWV method has been developed based on the realised law. Two procedures are suggested in this paper for PDF calculation based on the novel FCWV method, such as the trapezium approximation and the exponential function. The accuracy of the FCWV method has been verified.

The correctness of the law has been verified accurately, as shown in the results presented in Fig. 4.1. At discrete cells of varying cell weights over time, probabilities with 10,000 LHS result points remain constant and match the constant probabilities of cells that were determined initially. Two exceptions of slight deviations in the last cells of crack length at years 50 and 60 were observed. However, the main reason for these deviations is caused by extrapolation of $K_{I,l}$ solution beyond its validity limit, which is related to the fracture mechanics problem.

Crack length and depth PDFs have been regenerated over time for growing cracks, as shown in Figs. 4.2 and 4.3. The shapes of the PDFs for crack length and the depth evolve independently of each other. However, the associated crack length of a crack depth in a cell is in the corresponding crack length cell number at a point where cumulative probabilities match between crack depth and length. Eq. (2.5) can be applied to define the matching point of a crack length for a given crack depth (or vice versa). This finding is important, especially when calculating the probabilistic limit load in the future. In general, obtaining PDFs in a critical cell at a given time is sufficient. The critical cell may vary over time as the cracks grow larger and the following cell will become critical, or the PDFs of the

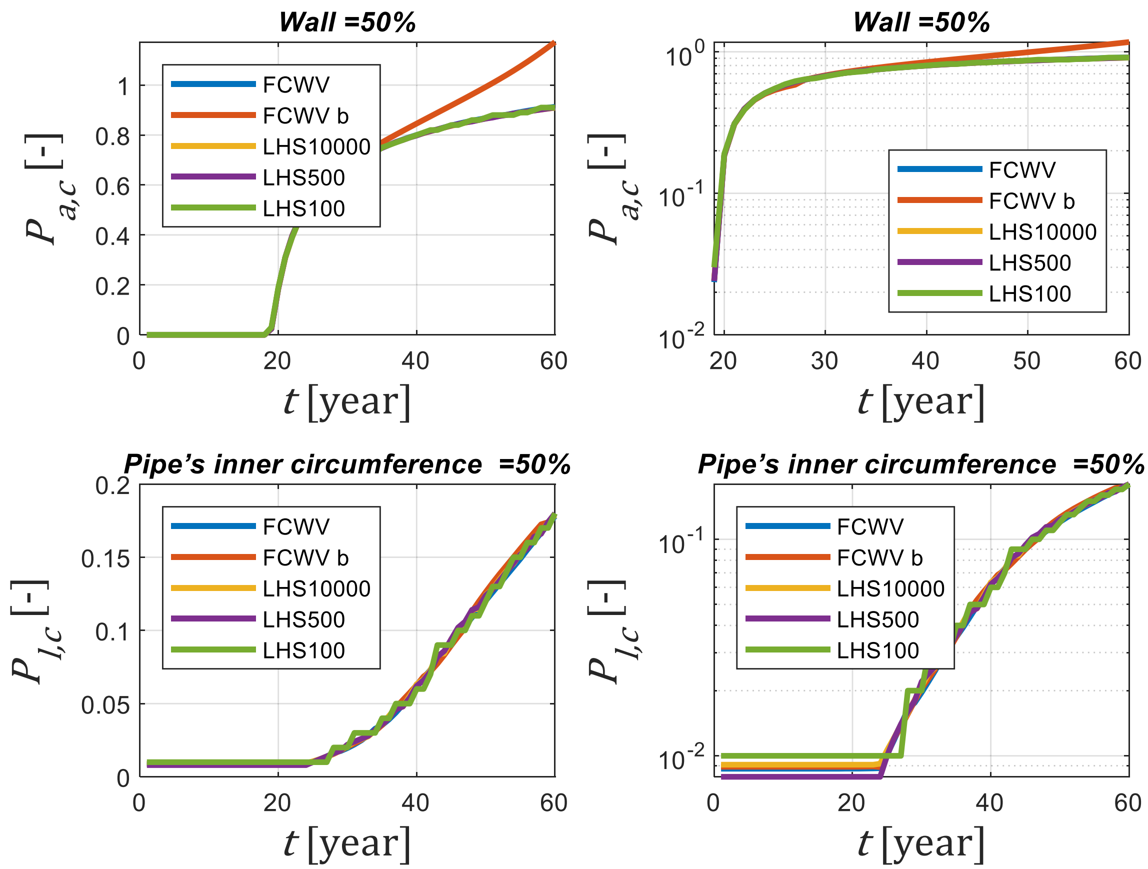

Fig. 4.10. Time-dependent cumulative probabilities of cracks reaching 50% of wall in the depth direction and 50% of inner circumference in the length direction.

critical cell may vary due to variations in the weight.

A correct cumulative probability estimation up to the critical crack size is essential in probabilistic leak or failure assessments. Thus, cumulative probabilities are estimated at different crack depths and lengths as a function of time with the FCWV method, and the results are verified with 10,000, 500 and 100 LHS result points, as shown in Figure 4.5 to Figure 4.10. Excellent agreement between the FCWV method ("FCWV") and 10,000 LHS result points ("LHS10000") can be observed in Figs. 4.5 to 4.10, where the computational time of the former is at most 1 % of the computational time of the latter. However, slight divergence in the FCWV method results in equal initial weight discretisation ("FCWV b") can be seen. This divergence was expected because of the sharp increase in the probabilities of the cells as a result of equal weights and the initial exponential PDF. The discretisation of the cells according to equal probabilities shall be performed to avoid such divergence (see Fig. 2.3). In the assessment of extremely low probability or some other special cases, the initial cell discretisation shall be performed based on the regions of interest.

In this paper, extreme loading conditions were considered in the analyses to verify the FCWV method firmly (because the sensitivity to the method and the number of discretised cells is considerably less in normal NPP loading conditions). Thus, approximately 10 cells with equal probabilities in the normal NPP loading conditions may be sufficient in the probabilistic pipe leak and break assessments.

By applying the FCWV method in the probabilistic crack growth analysis, efficiency is improved in terms of the computational time, disc space and obtaining results. Thus, other uncertain parameters, such as material properties and environment, can be included in the probabilistic crack growth assessment (without performing billions of analyses in a single time step). In real NPP conditions, cracks may initiate at any given time, with some probability. Hence, some assessments may require considering crack initiations with probabilistic initial sizes at different time steps. Therefore, assessing the growth of initiated cracks at different times up to the target time may easily lead to data explosion if traditional methods, such as LHS, are applied. Thus, the FCWV method can be the only practical method of choice in such scenarios. Finally, any natural phenomenon that grows over time and follows a law similar to the 'PDF law for growing cracks' can be analysed with the FCWV method much faster and more efficiently than with the other existing methods.

The FCWV method can be applied in PFM assessments with other input parameters probabilistically defined if continuous growth and size constraint conditions are maintained. Thus, the FCWV method requires further verification with other probabilistic input parameters related to material, loading and environment. Therefore, two more articles on the FCWV method will be written. The FCWV method will be verified separately in one article for each probabilistic input parameter. Indeed, such an approach will keep the random variable (crack depth or length) a one-dimensional problem over time. Another article will involve probabilistic treatment of a combination of different input parameters. Thus, the FCWV method will be developed for a multi-dimensional problem because the number of dimensions of the random variable must be the same as the number of probabilistic input parameters.

CRediT authorship contribution statement

Qais Saifi: Writing – original draft, Methodology, Investigation, Formal analysis, Conceptualization.

Declaration of Competing Interest

The authors declare that they have no known competing financial interests or personal relationships that could have appeared to influence the work reported in this paper.

Data availability

No data was used for the research described in the article.

Acknowledgements

VTT provided financial support for this study. I wish to express my gratitude to Mr. Otso Cronvall from VTT for proofreading and Mr. Paul Smeekes from TVO for expert cooperation in several projects, which eventually led me to realise the developed method.

References

[1] Antonio BA. Analysis of Ageing related events, JRC119754, 2020. http://doi.org/10.2760/239397.
[2] Khaleel MA, Simonen FA, Phan HK, Harris DO, Dedhia D. Fatigue Analysis of Components for 60-Year Plant Life, NUREG/CR-6674. USA: Pacific Northwest National Laboratory; June 2000.
[3] Brickstad B. WP-4, Review and benchmarking of SRMs and associated software. Appendix A1, SCC benchmark study, 5th Framework of the European Atomic Energy Community (EURATOM), NURBIM, Contract FIKS-CT-2001-00172, NURBIM Report D4/Appendix A1, May 2004.
[4] Hechmann K, Saifi Q. Comparative analysis of deterministic and probabilistic fracture mechanical assessment tools, p. 484–497, 2016. http://doi.org/10.3139/124.110725 KERNTECHNIK.
[5] Akihiro M, Yoshihito Y, Jinya K, Yinsheng L. Improvement of Probabilistic Fracture Mechanics Analysis Code PASCAL-SP Regarding Stress Corrosion Cracking in Nickel Based Alloy Weld Joint of Piping System in Boiling Water Reactor. J Press Vessel Technol 2022;144. https://doi.org/10.1115/1.4052449.
[6] Marie S, Chapuliot S, Kayser Y, Lacire MH, Drubay B, Barthelet B, et al. French RSE-M and RCC-MR code appendices for flaw analysis: Presentation of the fracture parameters calculation—Part III: Cracked pipes. Int J Press Vessels Pip May 2007;10(84). https://doi.org/10.1016/j.ijpvp.2007.05.005.
[7] International Atomic Energy Agency, Risk-Informed In-Service Inspection of Piping Systems of Nuclear Power Plants: Process, Status, Issues and Development, IAEA Nuclear Energy Series No. NP-T-3.1, 2010, Vienna. https://www.iaea.org/publications/8375/risk-informed-in-service-inspection-of-piping-systems-of-nuclear-power-plants-process-status-issues-and-development.
[8] Rahman S. Probabilistic fracture analysis of cracked pipes with circumferential flaws. Int J Press Vessels Pip 1997;70:223–36. https://doi.org/10.1016/S0308-0161(96)00034-8.
[9] Shittu AA, Kolios A, Mehmanparast A. A Systematic Review of Structural Reliability Methods for Deformation and Fatigue Analysis of Offshore Jacket Structures. Metals 2021;11:50. https://doi.org/10.3390/met11010050.
[10] Raynaud P, Kirk M, Benson M, Homiack M. Important Aspects of Probabilistic Fracture Mechanics Analyses, Technical Letter Report, TLR-RES/DE/CIB-2018-01, September 2018, U.S. NRC. https://www.nrc.gov/docs/ML1817/ML18178A431.pdf.
[12] Yoshimura S, Kanto Y. Probabilistic Fracture Mechanics for Risk-Informed Activities - Fundamentals and Applications. Probabilistic Fracture Mechanics Subcommittee: Atomic Energy Research Committee, The Japan Welding Engineering Society; March 2020. http://www-it.jwes.or.jp/ae/index.jsp.
[13] Rudland D, Scott P, Kurth R, Cox A. Continuing development of pro loca for the prediction of break probabilities for loss-of-coolant accidents, PVP2009-77053, July 2009, Czech Republic. https://doi.org/10.1115/PVP2009-77053.
[14] Scott P, Kurth R, Cox A, Olson R, Rudland D. Development of the PRO-LOCA Probabilistic Fracture Mechanics Code, MERIT Final Report, SSM, 2010:46 ISSN: 2000-0456, December 2010. http://www.stralsakerhetsmyndigheten.se/Global/Publikationer/Rapport/Sakerhet-vid-karnkraftverken/2010/SSM-Rapport-2010-46.pdf.
[15] Metropolis N, Ulam S. The Monte Carlo Method. J Am Stat Assoc 1949;44:335. https://doi.org/10.2307/2280232.
[16] Huang HZ, Gao H, Zhang X. Total fatigue life prediction for welded joints based on initial and equivalent crack size determination. Int J Damage Mech 2018;27(7):1084–104. https://doi.org/10.1177/1056789517723171.
[17] Mikheevskiya S, Glinkaa G, Cordesb T. Total life approach for fatigue life estimation of welded structures, 3rd International Conference on Material and Component Performance under Variable Amplitude Loading, VAL2015, Procedia Engineering 101, 2015, p. 177–184. https://doi.org/10.1016/J.PROENG.2015.02.023.
[18] Lee D, Huang Y, Achenbach JD. Probabilistic Analysis of Stress Corrosion Crack Growth and Related Structural Reliability Considerations. J Appl Mech. Feb 2016;83(2):21003 (9 pages), https://doi.org/10.1115/1.4031899.
[19] Bershak S, Kurgan V, Sydorenko I, Levinskyi O, Yeputatov Y. Probabilistic Analysis of Corrosion Fatigue Resistance, Advanced Manufacturing Processes III. InterPartner 2021, 2022, LNME, p. 250–259. https://doi.org/10.1007/978-3-030-91327-4_25.
[20] Harris DO, Dedhia D. WinPRAISE 07 Expanded PRAISE Code in Windows. USA: Structural Integrity Associates; January 2009.
[21] Bogdanov S, Mikheevskiy S, Glinka G. Probabilistic Analysis of the Fatigue Crack Growth Based on the Application of the Monte-Carlo Method to Unigrow Model. Mater Perform Charact 2014;3(3):214–31. https://doi:10.1520/MPC20130066.
[22] Dooyoul L, Dongin L, Hwasoo K, Seil B. Bayesian method for estimating initial cracks size distribution for probabilistic risk analysis of repairable structural details. Fatigue Fract Engng Mater Struct May 2022;45(8):2356–70. https://doi:10.1111/ffe.13751.